Geoscience Frontiers 12 (2021) 1010–1017

HOSTED BY

Contents lists available at ScienceDirect

Geoscience Frontiers

journal homepage: www.elsevier.com/locate/gsf

Research Paper

Chemical transformations of *n*-hexane and cyclohexane under the upper mantle conditions

Xin Yang, Yapei Li, Yajie Wang, Haiyan Zheng *, Kuo Li, Ho-kwang Mao

Center for High Pressure Science and Technology Advanced Research, Beijing, 100094, China

ARTICLE INFO

Keywords:
Alkanes
High pressure and high temperature
Dehydrogenation
Hydrocarbon
Upper mantle conditions

ABSTRACT

Alkanes are an important part of petroleum, the stability of alkanes under extreme conditions is of great significance to explore the origin of petroleum and the carbon cycle in the deep Earth. Here, we performed Raman and infrared (IR) spectroscopy studies of *n*-hexane and cyclohexane under high pressure up to ~42 GPa at room temperature (RT) and high temperature (HT). *n*-Hexane and cyclohexane undergo several phase transitions at RT around 1.8, 8.5, 18 GPa and 1.1, 2.1, 4.6, 13, 30 GPa, respectively, without any chemical reaction. By using resistive heating combined with diamond anvil cell at pressure up to 20 GPa and temperature up to 1000 K, both *n*-hexane and cyclohexane decompose to hydrogenated graphitic carbon and *n*-hexane exhibits higher stability than cyclohexane. Our results indicate that hydrocarbons tend to dehydrogenate in the upper mantle, and the extension of carbon chains may lead to the formation of some unsaturated compounds and eventually transfer into graphitic products.

1. Introduction

The behavior of C-H system under high pressure and high temperature conditions is of great importance in many fields like organic chemistry, planetary and Earth sciences because they are one of the major components of giant planets and also involved in the C-H circulation at the reduction conditions in the deep Earth. Many theoretical and experimental results on the physical and chemical transition process of methane have been reported. It was predicted that CH_4 dissociated into the diamond and hydrogen above 300 GPa (Ancilotto et al., 1997). Using the Evolutionary Xtallography (USPEX) method, Gao et al. (2010) found that CH_4 polymerizes into ethane (C_2H_6) and butane (C_4H_{10}) under high pressure, which further dissociate into diamond and hydrogen. By performing the *ab* initio molecular dynamic simulations and free energy calculations, Spanu et al. (2011) figured out that the advanced alkanes become more stable when the pressure is above 4 GPa and the temperature is between 1000 K and 2000 K, which corresponds to the depths of >120 km.

Experimentally, laser heating diamond anvil cells experiments showed that diamond and polymeric hydrocarbons formed at pressures of 10–50 GPa and temperatures of 2000–3000 K (Benedetti et al., 1999). Kolesnikov et al. (2009) further suggested that methane transformed into ethane, propane and butane under upper-mantle conditions (2 GPa and 1000–1500 K). By heating the methane at the pressure higher than 24 GPa and temperatures over 1500 K, the elementary carbon, heavier alkanes and unsaturated hydrocarbons were formed (Lobanov et al., 2013). The above theoretical and experimental facts indicate that methane is not stable and transforms into heavy hydrocarbons at pressure above 2 GPa and temperature above 1000 K. That means heavy hydrocarbons may play a critical role in the C-H liquids under the upper and deep mantle conditions, which were still poorly understood.

Thus, in order to understand the carbon reservoirs and fluxes in the deep Earth, in this manuscript, through the combination of resistance heating and in situ Raman spectroscopy, we explored phase transitions and chemical reactions of two alkanes with medium chain-length and cyclic molecules, *n*-hexane (C_6H_{14}) and cyclohexane (C_6H_{12}), up to 20 GPa and 1000 K, which corresponds to the upper mantle conditions, about 610 km depth in the deep Earth. Their stabilities under room temperature and high pressure were also investigated. The results show that *n*-hexane and cyclohexane are stable at room temperature up to at least 42 GPa. Under high temperature and high pressure, a form of hydrogenated graphitic carbon was obtained at last, which shows that

* Corresponding author.
E-mail addresses: xin.yang@hpstar.ac.cn (X. Yang), yapei.li@hpstar.ac.cn (Y. Li), yajie.wang@hpstar.ac.cn (Y. Wang), zhenghy@hpstar.ac.cn (H. Zheng), likuo@hpstar.ac.cn (K. Li), maohk@hpstar.ac.cn (H.-k. Mao).

Peer-review under responsibility of China University of Geosciences (Beijing).

https://doi.org/10.1016/j.gsf.2020.06.006
Received 15 November 2019; Received in revised form 25 May 2020; Accepted 20 June 2020
Available online 7 August 2020

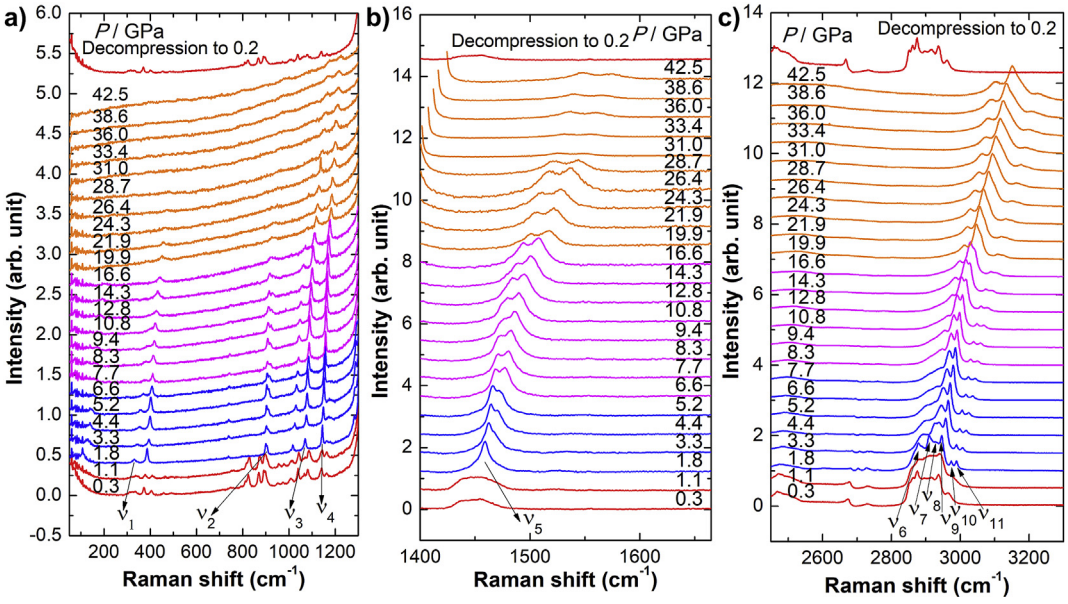

Fig. 1. Raman spectra of *n*-hexane with increasing pressure from 0.3 GPa to 42.5 GPa and decompressed from 42.5 GPa.

alkanes tend to dehydrogenate and polymerize under extreme conditions. For carbon atoms, this is a process of transition from saturated alkanes to unsaturated ones. Temperature and pressure can affect the degree of dehydrogenation and the final products. Our research provides insights into the stabilities and chemical reactions of simple alkanes with medium-length chains under high temperature and high pressure conditions and provides a reference for the origin of petroleum with the transportation and transformation of hydrocarbon fluids in the deep Earth.

2. Experimental methods

2.1. Materials and high pressure and high temperature generation

n-Hexane (97%) and cyclohexane (99.5%) were purchased from Macklin and used without further purification. A symmetric diamond anvil cell (DAC) with an anvil culet size of 300 μm in diameter was applied for the in situ high pressure Raman and infrared (IR) measurements at room temperature. For the in situ IR measurement, the type-IIa diamond anvils were used to avoid the absorption in the range of 1000–1300 cm^{-1}. *n*-Hexane and cyclohexane were loaded into the holes with d = 150 μm drilled on the T-301 stainless steel gaskets which were pre-indented to ~30 μm in thickness. Pressure was determined by measuring ruby fluorescence, according to equation P (GPa) = 248.4 $[(\lambda/\lambda_0)^{7.665} - 1]$ (Mao et al., 1986). A BX90 DAC with an anvil culet size of 300 μm in diameter combined with resistance heating was used for the in situ high temperature and high pressure experiments. A resistive ring heater was mounted around the diamond, and the temperature is measured by a K-type thermocouple attached to the diamond. Pressure was determined by measuring the temperature-corrected ruby fluorescence (Rekhi et al., 1999). Tungsten gaskets were pre-indented to ~30 μm in thickness and center holes with d = 90 μm were drilled to serve as a sample chamber. All of samples were loaded in liquid at room temperature and compressed to ~20 GPa before heating.

2.2. In situ Raman and IR spectroscopy measurements

Raman experiments were carried out on a Renishaw Raman microscope (RM1000). The 532 nm line of a Nd:YAG laser was used as the excitation source. The Si line was used to calibrate the system before measurement. The high-pressure in situ IR spectra were collected in transmission mode in the range of 600–4000 cm^{-1} on a Bruker VERTEX 70v FTIR spectrometer with a HYPERION 2000 microscope. A Globar was used as a conventional source. The resolution was 2 cm^{-1} and the 20 μm × 20 μm aperture was chosen to select the measured sample area. The background of the IR measurements was collected from empty DAC in the aperture region before loading sample. During the IR measurement, N_2 was flowed in the optical path to try to remove the moisture and carbon dioxide in the air.

Table 1
Frequencies and assignments of the Raman modes of *n*-hexane at 1.8 GPa and room temperature.

Phase I (1.8 GPa)	assignments
331	ν_1 (LAM C–C–C angle bending)
906	ν_2 (methyl rocking mode, GTT)
1070	ν_3 (C–C stretching, GTT + TGT)
1144	ν_4 (–CH_3 rocking + C–C stretching, TTT + TGT)
1459	ν_5 (asymmetric > CH_2 and -CH_3 bending + >CH_2 rocking + CH_3 deformation and CH_2 scissoring)
2878	ν_6 (symmetric > CH_2 stretching, TTT)
2910	ν_7 (symmetric > CH_2 stretching, TTT)
2927	ν_8 (symmetric > CH_2 stretching, TGT)
2946	ν_9 (in-plane asymmetric methyl stretching, TTT)
2974	ν_{10} (out-plane asymmetric methyl stretching, GTT)
2989	ν_{11} (asymmetric C–H methyl stretching, TTT)

3. Results and discussion

3.1. n-Hexane

3.1.1. Compression under high pressure and room temperature

We studied *n*-hexane at room temperature up to 42.5 GPa using in situ Raman and IR spectroscopy. As shown in Fig. 1, when compressing the *n*-hexane slowly from 0.3 GPa to 1.8 GPa, all the peaks become sharper and several peaks including 409, 829, 874, 1039, 1043, and 1087 cm^{-1} disappeared, which corresponds to the phase transition from liquid to solid state, phase I. Assignments of the Raman modes of *n*-hexane at 1.8 GPa were summarized in Table 1 according to the literature (Kavitha and Narayana, 2007). Upon compression, a weak new peak was observed at 2948 cm^{-1} at 8 GPa and slight discontinuity was shown in the plots of the

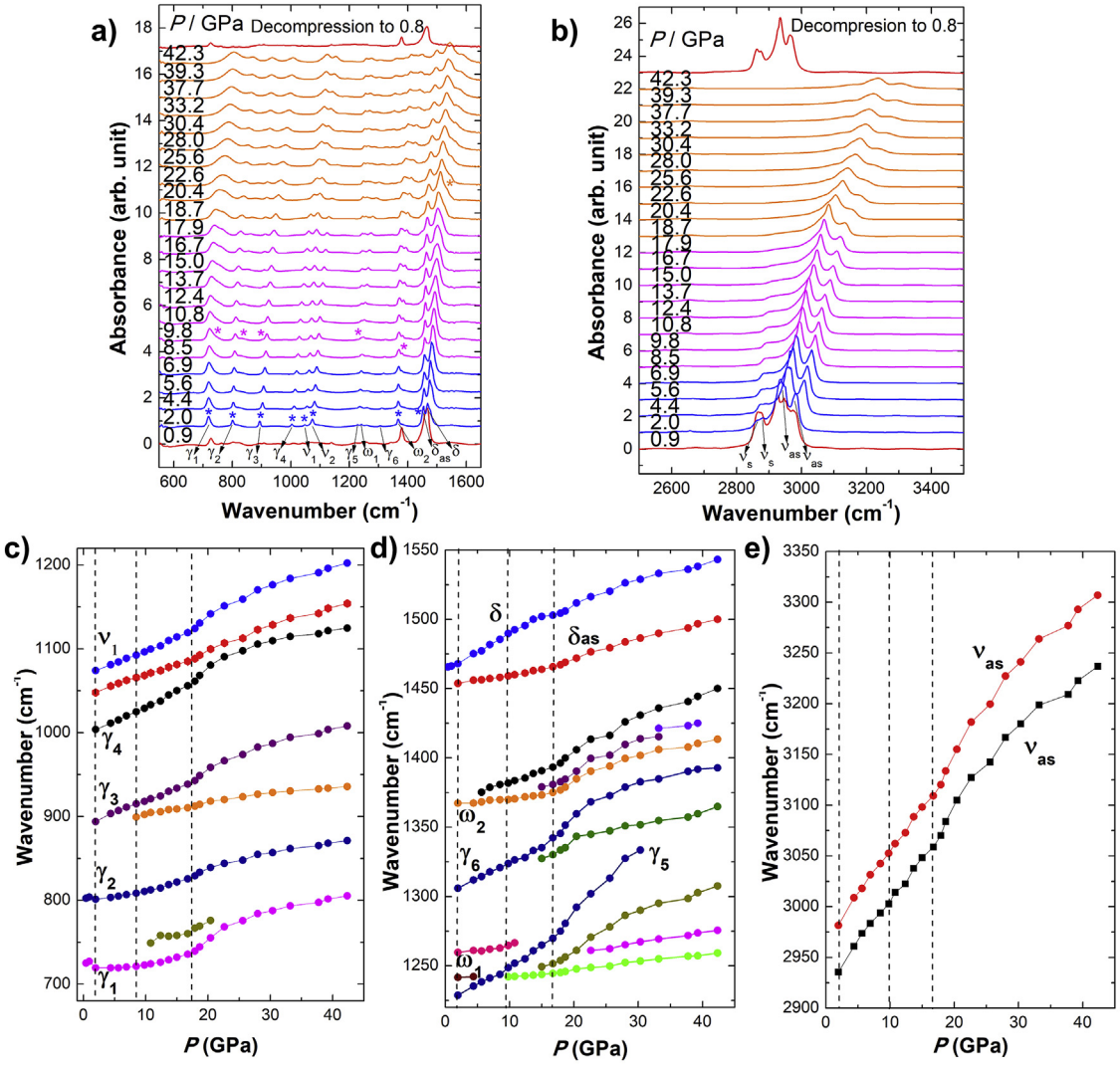

Fig. 2. IR spectra of *n*-hexane with increasing pressure from 0.3 GPa to 42.3 GPa (a) and decompressing from 42.3 GPa (b). The new peaks are indicated by asterisks. (c), (d) and (e) Frequency shifts of IR modes as a function of pressure. Dotted lines represent the phase boundaries.

Table 2
Assignments of IR frequencies of *n*-hexane at 1.9 GPa and room temperature.

Phase I (1.9 GPa)	Assignments
719	γ_1 (rocking-twisting CH_2)
801	γ_2 (rocking-twisting CH_2)
893	γ_3 (rocking CH_3)
1003	γ_4 (rocking-twisting CH_2)
1048	ν_1 (C-C stretching)
1073	ν_2 (C-C stretching)
1228	γ_5 (twisting-rocking CH_2)
1241	ω_1 (wagging CH_2)
1306	γ_6 (twisting-rocking CH_2)
1367	ω_2 (wagging CH_2)
1454	δ_{as} (asymmetric CH_3 deformation + CH_2 deformation)
1475	δ (CH_2 deformation)
2863	ν_s (symmetric C–H stretching CH_2)
2880	ν_s (symmetric C–H stretching CH_3)
2935	ν_{as} (asymmetric C–H CH_2)
2974	ν_{as} (asymmetric C–H CH_3)
2981	ν_{as} (asymmetric C–H CH_3)

pressure dependence of various Raman modes at around 7 GPa and 20 GPa, which indicates there might be a phase transition from I to II and II to III (Fig. S1). More solid evidence about the phase transition of *n*-hexane under high pressure is from IR spectroscopy. As shown in Fig. 2, upon compressing to 2.0 GPa, *n*-hexane shows the transition from liquid to solid state (phase I), with the peaks becoming sharper and several new IR modes like 719, 800, 894, 1004, 1074, 1368 and 1453 cm^{-1} (marked by blue asterisks) appearing. Assignments of IR modes of phase I at 1.9 GPa were shown in Table 2 according to previous researches (Snyder, 1965; Yamaguchi et al., 2003). At 8.5 GPa, a new peak was observed on the high frequency side of CH_2-wag and several new peaks including 745, 901 and 1234 cm^{-1} were detected, corresponding to the phase transition from phase I to II. The intensities of these peaks increased when compressing to higher pressure. By further analyzing the pressure dependence of various IR modes of *n*-hexane, most of them show obvious discontinuity at around 18 GPa, indicating the phase transition from II to III. Phase III is stable up to 42.5 GPa, the maximum pressure investigated in this work. After decompression to ambient pressure, the Raman and IR patterns of the sample are similar to those before compression, indicating that the transitions are reversible and *n*-hexane is stable to at least 42 GPa at room temperature.

3.1.2. *Investigation under high pressure and high temperature*

Based on the room temperature studies, we investigated the chemical transformation of *n*-hexane under high temperature and high pressure. During the heating process, the pressure in the sample chamber first

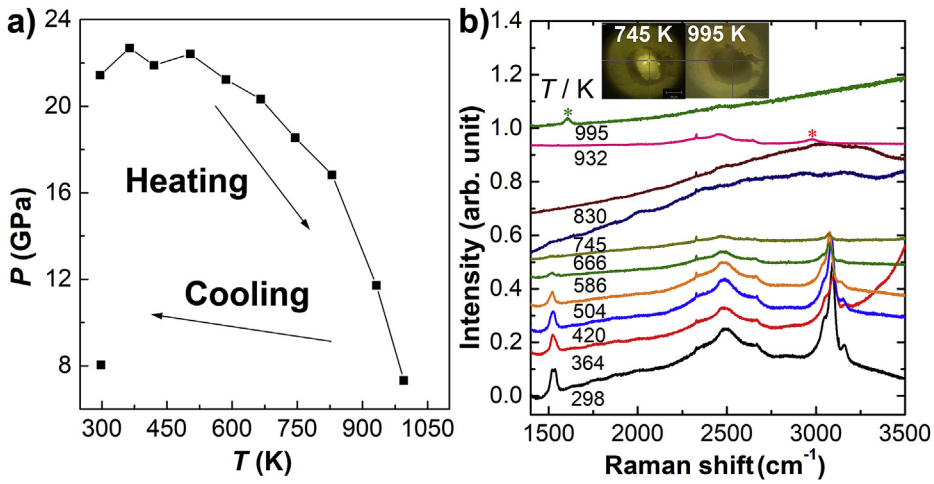

Fig. 3. (a) Temperature and pressure curve during the heating process of *n*-hexane. (b) Selected Raman spectra of *n*-hexane with increasing temperature at 21.4 GPa. The new peaks are indicated by the asterisks. The insets are microphotographs of the sample chamber at 745 K and 995 K, respectively, by Raman microscope.

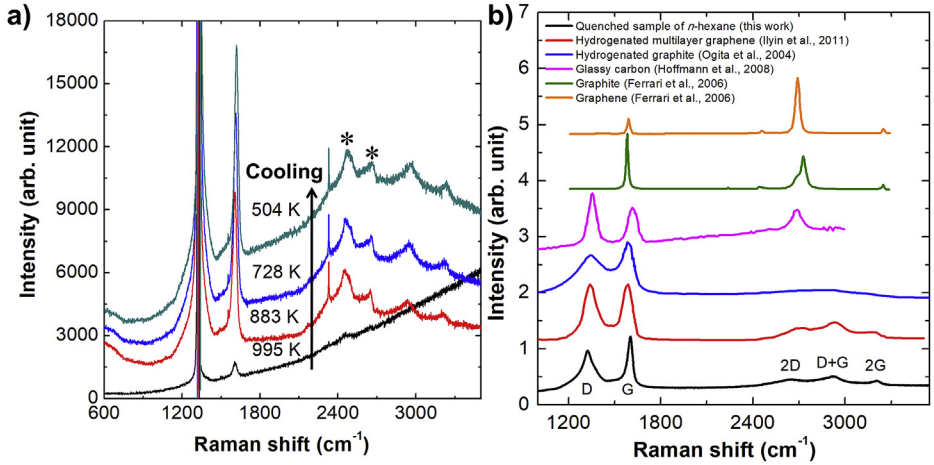

Fig. 4. (a) Raman spectra of *n*-hexane during cooling. The second order Raman of diamonds are indicated by the asterisks. (b) Raman spectra of quenched sample outside diamond anvil cells.

increased to ~23 GPa from 21.4 GPa and then decreased significantly. The temperature and pressure variations of the whole process are shown in Fig. 3a. The intensity of each Raman peak gradually decreases (Fig. 3b) upon heating. When heating to 745 K, strong fluorescence appeared and obscured the Raman signals of $–CH_2$ and $–CH_3$ bending vibrations as well as sp^3 C–H stretching vibration (Fig. 3b), which lasts to 830 K. The appearance of fluorescence suggests that *n*-hexane underwent a dehydrogenation process to produce conjugated structures like aromatics or conjugated alkenes. At 932 K and 11.7 GPa, the fluorescence of the sample disappeared with a weak single peak appeared at 2978 cm^{-1}, corresponding to sp^3 C–H stretching (Fig. 3b). For comparison, the Raman spectrum of *n*-hexane under this pressure and room temperature shows five peaks at 2971, 2997, 3011, 3054 and 3074 cm^{-1}, respectively, which suggests a different alkane was produced upon heating.

When heating to 995 K, the sample was still transparent at first. However, after being irradiated by the 532 nm laser of the Raman spectrometer, the sample suddenly became opaque (Fig. 3b) and showed strong fluorescence that saturated the detector. Subsequently, after a couple of minutes at the same pressure and temperature, the fluorescence disappeared with a new weak peak appeared at 1606 cm^{-1}, indicating the formation of extended carbon structure (Fig. 3b). This is a process of dehydrogenation from alkane to conjugated hydrocarbon, and then to some carbon-based species. This process is basically initiated by thermal activation and could be promoted by laser. Upon cooling, the intensity of the peak at 1606 cm^{-1} increases rapidly and three new peaks appear at 2669, 2933 and 3211 cm^{-1} (Fig. 4a), which suggests the reaction is still going on after initiation even if it is cooling down by several hundred degrees.

In the whole heating process, due to the strong ruby signal, we could not observe the hydrogen signal in the region of 4000–5000 cm^{-1}. After cooling, the sample chamber became larger, which allowed us to avoid the ruby signal. However, we didn't find any hydrogen signal either. The signal of hydrogen was not reported in previous studies of octane, decane, octadecane and nonadecane under 10–20 GPa, 3000 K either (Zerr et al., 2006). This should be attributed to the diffusion of hydrogen under high temperature, which may intercalate into the metallic gasket or even diamond under high pressure and high temperature and reaction is actually in an open system. In previous report about the dissociation of CH_4 under high pressure and high temperature conditions, Benedetti et al. did not observe the Raman-active stretching mode of H_2, but they found the lattice parameters of rhenium was expanded as much as 2.6% which provides indirect evidence that hydrogen was produced and intercalated to the rhenium gasket (Benedetti et al., 1999). In fact, hydrogen signals are very difficult to capture in high temperature and high pressure systems, which require more thorough and detailed investigations.

The Raman spectra of the quenched sample outside diamond anvil cells (Fig. 4b) showed significant D band at ~1320 cm^{-1} and G band at

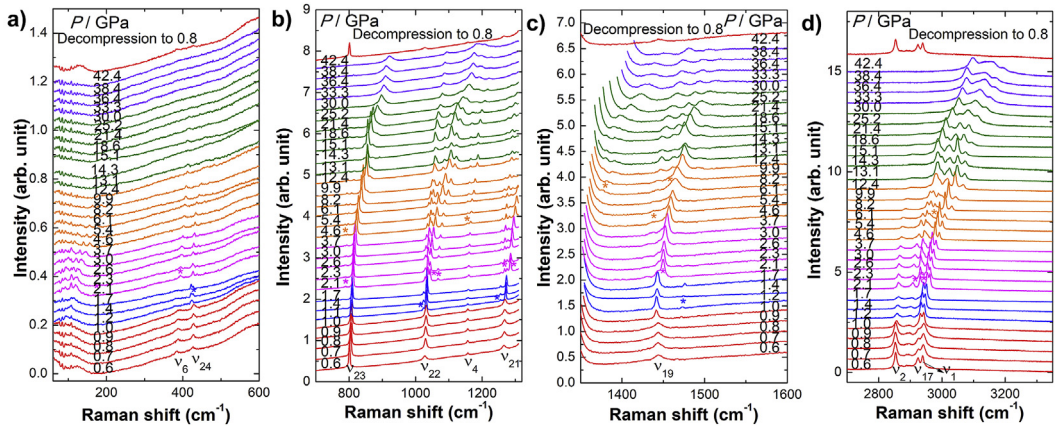

Fig. 5. Raman spectra of cyclohexane with increasing pressure from ambient pressure to 42 GPa and decompressing from 42 GPa.

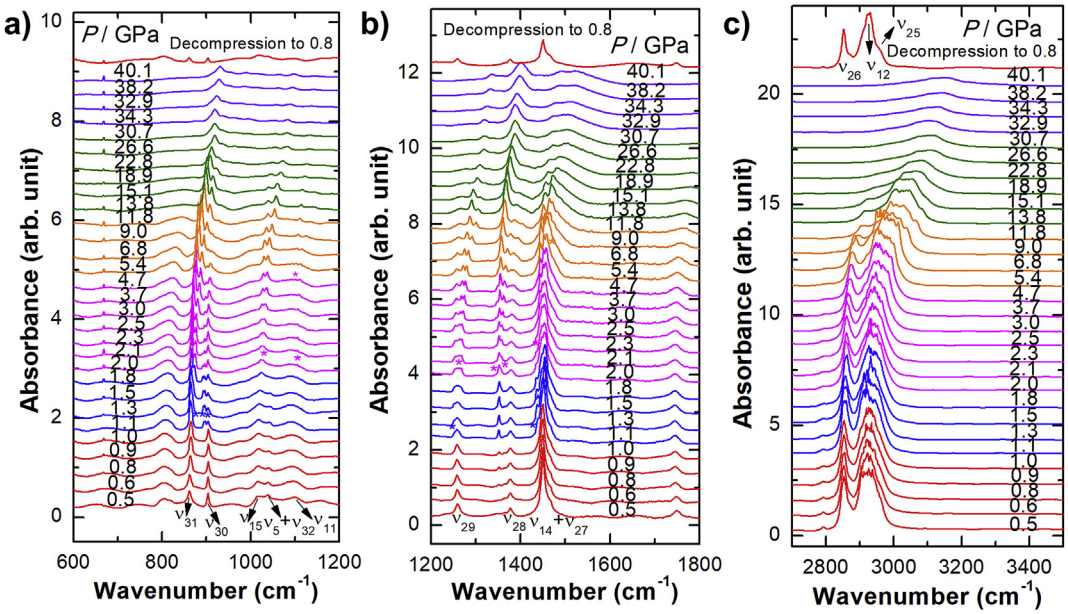

Fig. 6. IR spectra of cyclohexane with increasing pressure from ambient pressure to 40 GPa and decompressing from 40 GPa.

~1600 cm^{-1}. In addition, the peaks at 2648, 2923 and 3208 cm^{-1} are classified as 2D band, D + G or 2G band respectively. To analyze our products, we compared it to the Raman spectra of graphite, hydrogenated graphite, glassy carbon, graphene, hydrogenated graphene and hydrogenated amorphous carbons. Highly oriented graphite exhibits sharp G band at ~1580 cm^{-1}, 2D band consisting of multiple peaks at ~2710 cm^{-1}, and peaks at ~2450 cm^{-1}, ~3250 cm^{-1} in the second order spectrum, while disordered graphite and glassy carbon show a D band at ~1370 cm^{-1} (Nemanich and Solin, 1979; Reich and Thomsen, 2004; Hoffmann et al., 2008). In hydrogenated graphite, the D band is strong, the G band becomes broad and the second order Raman becomes weak (Ogita et al., 2004). Graphene also exhibits sharp G band and 2G band. The 2G band gradually widened with the increasing of layers and shows hardly distinguishable Raman spectra of graphite when the number of layers exceeds 5 (Ferrari et al., 2006). After hydrogenation, D band, D′ band at ~1620 cm^{-1} and D + D′ or D + G band at ~2920 cm^{-1} were observed, with the 2D peak widened and its intensity decreased (Elias et al., 2009; Luo et al., 2009). The similar Raman spectra of hydrogenated multilayer graphene were presented by Ilyin et al. (2011). Hydrogenated amorphous carbon has a wide G band at ~1560 cm^{-1} and a weak D band at ~1360 cm^{-1} (Ferrari and Robertson, 2000; Casiraghi et al., 2005). After annealed at high temperature, the G band narrows and blue shifts to ~1600 cm^{-1} with the D band intensity increases, which are explained by the formation of larger aromatic clusters in the material at high temperature (Pardanaud et al., 2013). As shown in Fig. 4b, by comparing the carbon materials above, we concluded our products were hydrogenated graphitic carbon, an intermediate between alkane and graphite, which is caused by incomplete dehydrogenation pyrolysis.

Table 3
Frequencies and assignments of the Raman modes of cyclohexane at 0.6 GPa and room temperature.

Phase I (0.6 GPa)	Assignments
385	ν_6 (C–C–C deformation + C–C torsion)
427	ν_{24} (C–C–C deformation + C–C torsion)
801	ν_{23} (CH_2 rocking)
1027	ν_{22} (C–C stretching)
1157	ν_4 (CH_2 rocking)
1265	ν_{21} (CH_2 twisting)
1444	ν_{19} (CH_2 scissoring)
2854	ν_2 (symmetric > CH_2 stretching)
2888	ν_{18} (symmetric > CH_2 stretching)
2925	ν_{17} (asymmetric > CH_2 stretching)
2939	ν_1 (asymmetric > CH_2 stretching)

Table 4
Assignments of IR frequencies of cyclohexane at 0.8 GPa and room temperature.

Phase I (0.5 GPa)	Assignments
863	ν_{31} (C–C stretching)
903	ν_{30} (CH_2 rocking)
1037	$\nu_5 + \nu_{32}$ (C–C stretching + torsion)
1098	ν_{11} (CH_2 twisting)
1259	ν_{29} (CH_2 twisting)
1378	ν_{28} (CH_2 wagging)
1450	ν_{14}, ν_{17} (CH_2 scissoring)
2853	ν_{26} (symmetric > CH_2 stretching)
2923	ν_{12} (symmetric > CH_2 stretching)
2953	ν_{25} (asymmetric > CH_2 stretching)

3.2. Cyclohexane

3.2.1. Compression at high pressure and room temperature

For comparison, we also studied cyclohexane as a representative of cycloalkanes. The phase transition of cyclohexane at room temperature up to ~42 GPa was investigated by Raman and IR spectroscopy (Figs. 5 and 6). Cyclohexane solidifies into phase I < 0.5 GPa (Haines and Gilson, 1989). Assignments of the Raman modes of cyclohexane at 0.6 GPa were summarized in Table 3 according to previous studies (Haines and Gilson, 1989; Crain et al., 1992). At 1.2 GPa, four new peaks appeared around 400, 1024, 1256 and 1473 cm^{-1} respectively, suggesting a new phase, phase III, emerged, which is distinguished from the phase II observed below 186 K (Kahn et al., 1973). Above 2.1 GPa, a new peak centered at 120 cm^{-1} emerged in the region of lattice modes. Meanwhile, several new peaks appeared at 395, 788, 1043, 1067, 1268, 1285, 1449, 2909, 2930, and 2936 cm^{-1}. The intensities of the original peaks corresponding to the ν_{19} and ν_{21} decreased. All of these are attributed to the phase transition from III to IV. The phase transition from IV to V at 4.6 GPa is evidenced by the emergence of the new peaks at 787, 1155, and 1437 cm^{-1}. When compressing to higher pressure, four new peaks including 1376, 1438, 1453, and 2969 cm^{-1} appeared which is also attributed to the phase transition from IV to V. Upon further compression, the obvious discontinuities were observed at 13 GPa and 30 GPa, which may indicate another two phase transitions from V to VI and from VI to VII (Fig. S2), that is consistent with previous report (Pravica et al., 2004). Such evidence of phase transition was also observed in the IR spectra. According to previous studies, assignments of the IR modes of cyclohexane at 0.8 GPa were summarized in Table 4 (Miller and Golob, 1964; Haines and Gilson, 1989). At 1.1 GPa, six new peaks were observed at 867, 894, 897, 1252, 1439, and 1448 cm^{-1}, corresponding to the change of phase I to phase III. After compression to about 2 GPa, six new peaks at 1028, 1105, 1267, 1343, 1357, and 1442 cm^{-1} appeared, indicating the formation of phase IV. In addition, peaks at 1100 and 1462 cm^{-1} occurred near 5 GPa, consistent with the phase transition observed in Raman spectrum at 4.6 GPa. Like *n*-hexane, cyclohexane shows the same spectrum as the starting material after decompression from 42 GPa to ambient conditions, which means it is stable at room temperature up to at least 42 GPa.

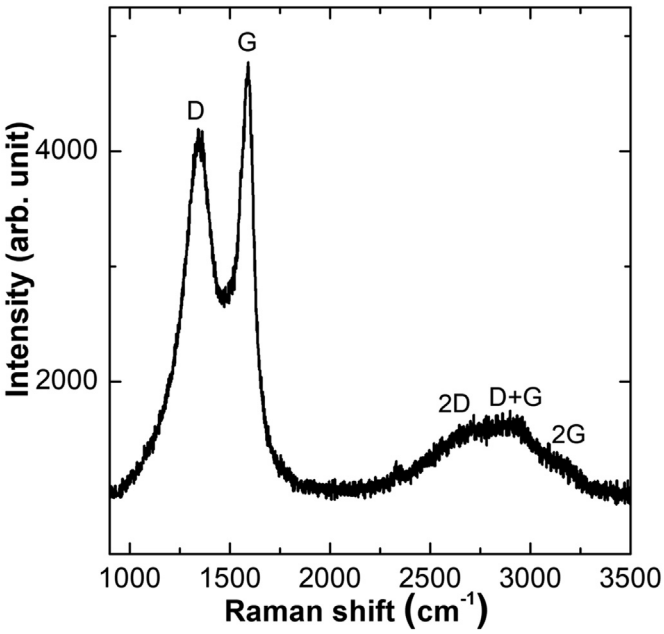

Fig. 8. Raman spectra of quenched cyclohexane after resistance heating.

3.2.2. Investigation under high pressure and high temperature

During heating, we also recorded the pressure at each temperature point. The pressure rose to 21.1 GPa when the temperature was 334 K and then decreased gradually (Fig. 7a), which explained the red shifts of the Raman peaks of cyclohexane during heating (Fig. 7b and c).

Similar to *n*-hexane, as the temperature increases, the intensities of Raman peaks gradually decrease. However, no strong fluorescence was observed during the heating process, indicating a completely different reaction path. Around 818 K, almost all the Raman peaks disappeared, only a very weak bulge was observed around 3000 cm^{-1}. After heating to 873 K, the sample quickly becomes opaque, suggesting the occurrence of the reaction. No obvious laser-induced reaction was observed during this process.

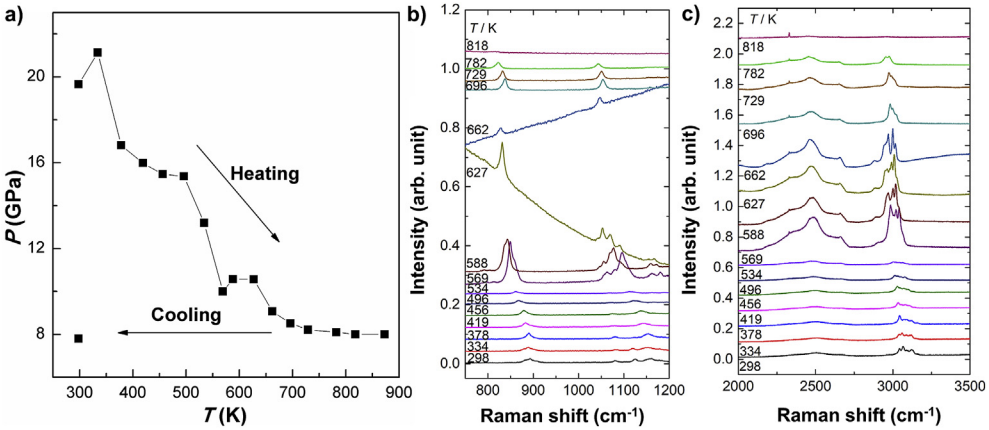

Fig. 7. (a) Temperature and pressure curve during the whole experiment of cyclohexane. (b, c) Selected Raman spectra of cyclohexane with increasing temperature at 19.7 GPa.

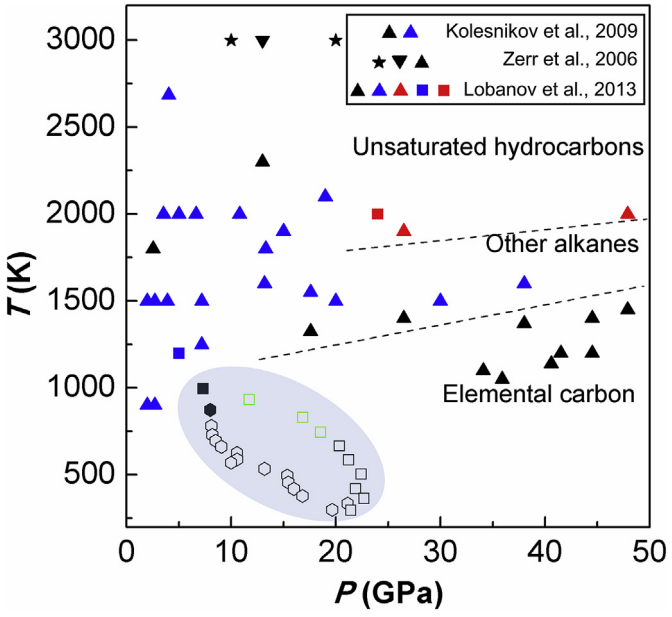

Fig. 9. C-H system experiment results under high temperature and high pressure with different staring materials. Upright triangles represent starting material is methane, inverted triangles represent ethane, squares represent *n*-hexane, hexagons represent cyclohexane and stars represent long-chain alkanes (C_8H_{18}, $C_{10}H_{22}$, $C_{18}H_{38}$ and $C_{19}H_{40}$). Different colors represent different products. Black represents the production of elemental carbon, blue represents the production of other short alkanes, and red represents the observation of unsaturated hydrocarbons. Black blank shapes represent that no reaction occurred, and the green blank squares indicates that fluorescence was observed. The thick dotted line summarizes the data of the chemical reactions of methane. Blue area represents the results of our experiments. Other results come from Zerr et al. (2006), Kolesnikov et al. (2009) and Lobanov et al. (2013).

After cooling to room temperature, some regions in DAC showed strong fluorescence, suggesting the formation of some complex conjugated hydrocarbons. The Raman of quenched sample (Fig. 8) showed significant broad D band (1348 cm^{-1}), G band (1590 cm^{-1}), 2D band (2705 cm^{-1}), 2G band (3153 cm^{-1}) and D + G band (2900 cm^{-1}), which is similar to the product of *n*-hexane. No signal of molecular hydrogen was observed throughout the experiment.

Those results suggest that cyclohexane and *n*-hexane undergo a decomposition-polymerization process under high temperature and high pressure, eventually forming an extended carbon structure. The decomposition tends to go through to the end after initiation and the hydrogen seems to leave the reaction system by diffusion, which promotes the shift of the chemical equivalence to the decomposed products. During this process, temperature and pressure conditions would affect the degree of dehydrogenation and some complex hydrocarbons may be produced. This is similar with the previous literatures which shows some dehydrogenation products were also observed in methane, ethane, *n*-hexane, and aromatic hydrocarbons (Davydov et al., 2004; Lobanov et al., 2013).

In Fig. 9, we summarized some results of alkanes under high temperature and high pressure. In the range of 2–20 GPa, the pyrolysis temperature of methane is higher than that of *n*-hexane and cyclohexane, while that of *n*-hexane is higher than cyclohexane, indicating that short-chain alkanes (with higher H/C ratio) are more thermally stable under upper mantle conditions. Our studies also suggest that, once the short alkane polymerized to form advanced hydrocarbons, the reaction would continue until the stable terminal products like graphitic species are formed. Additionally, under higher pressure, higher temperature would be needed for reaction, and some advanced alkanes and unsaturated compounds may be produced as intermediate on the way to graphitic product.

4. Conclusion

In summary, Raman and IR spectra of *n*-hexane and cyclohexane were studied up to ~42 GPa at room temperature. We observed a liquid-solid transition of *n*-hexane at 1.8 GPa and two solid-solid transitions around 8.5 GPa and 18 GPa. Cyclohexane has a more complex phase transition, which solidifies below 0.5 GPa and experiences five solid-solid transitions near 1.1, 2.1, 4.6, 13 and 30 GPa. By using resistive heating combined with in situ Raman spectroscopy, the reactions of *n*-hexane and cyclohexane under upper mantle conditions were explored for the first time. We obtained a product similar to hydrogenated graphitic carbon, which suggests that carbon atoms in alkanes tend to dehydrogenate and bond to other carbon atoms to form extended carbon structures under high temperature and high pressure. By comparing the pyrolysis temperatures of these two alkanes, we find that *n*-hexane is more stable than cyclohexane under high temperature and high pressure, which may be due to the higher saturation of *n*-hexane. Our study provides new insights to understand carbon reservoirs and fluxes in the deep Earth and also provides a reference for the study of alkanes with longer chains under extreme conditions. It is necessary to further characterize the composition and percentage of the complex products produced by alkanes under high temperature and high pressure.

Declaration of competing interest

The authors declare that they have no known competing financial interests or personal relationships that could have appeared to influence the work reported in this paper.

Acknowledgements

This study is funded by the National Key Research and Development Program of China (2019YFA0708502). The authors also acknowledge the support of the National Natural Science Foundation of China (NSFC) (Grant Nos. 21771011 and 21875006). The authors acknowledge the support from the Top 1000-Talents Award.

Appendix A. Supplementary data

Supplementary data to this article can be found online at https://doi.org/10.1016/j.gsf.2020.06.006.

References

Ancilotto, F., Chiarotti, G.L., Scandolo, S., Tosatti, E., 1997. Dissociation of methane into hydrocarbons at extreme (planetary) pressure and temperature. Science 275, 1288–1290.
Benedetti, L.R., Nguyen, J.H., Caldwell, W.A., Liu, H., Kruger, M., Jeanloz, R., 1999. Dissociation of CH_4 at high pressures and temperatures: diamond formation in giant planet interiors? Science 286, 100–102.
Casiraghi, C., Piazza, F., Ferrari, A.C., Grambole, D., Robertosn, J., 2005. Bonding in hydrogenated diamond-like carbon by Raman spectroscopy. Diam. Relat. Mater. 14, 1098–1102.
Crain, J., Poon, W.C.-K., Cairns-Smith, A., Hatton, P.D., 1992. High-pressure Raman spectroscopic study of cyclohexane C_6H_{12} and C_6D_{12}. J. Phys. Chem. 96, 8168–8173.
Davydov, V.A., Rakhmanina, A.V., Agafonov, V., Narymbetov, B., Boudou, J.-P., Szwarc, H., 2004. Conversion of polycyclic aromatic hydrocarbons to graphite and diamond at high pressures. Carbon 42, 261–269.
Elias, D.C., Nair, R.R., Mohiuddin, T.M.G., Morozov, S.V., Blake, P., Halsall, M.P., Ferrari, A.C., Boukhvalov, D.W., Katsnelson, M.I., Geim, A.K., Novoselov, K.S., 2009. Control of graphene's properties by reversible hydrogenation: evidence for graphene. Science 323, 610–613.
Ferrari, A.C., Meyer, J.C., Scardaci, V., Casiraghi, C., Lazzeri, M., Mauri, F., Piscanec, S., Jiang, D., Novoselov, K.S., Roth, S., Geim, A.K., 2006. Raman spectrum of graphene and graphene layers. Phys. Rev. Lett. 97, 187401.
Ferrari, A.C., Robertson, J., 2000. Interpretation of Raman spectra of disordered and amorphous carbon. Phys. Rev. B 61, 14095–14107.
Gao, G., Oganov, A.R., Ma, Y., Wang, H., Li, P., Li, Y., Iitaka, T., Zou, G., 2010. Dissociation of methane under high pressure. J. Chem. Phys. 133, 144508.
Haines, J., Gilson, D.F.R., 1989. Vibrational spectroscopic studies of the phase transitions in cyclohexane at high pressure. J. Phys. Chem. 93, 7920–7925.

Hoffmann, G.G., de With, G., Loos, J., 2008. Micro-Raman and tip-enhanced Raman spectroscopy of carbon allotropes. Macromol. Symp. 265, 1–11.
Ilyin, A.M., Guseinov, N.R., Tsyganov, I.A., Nemkaeva, R.R., 2011. Computer simulation and experimental study of graphane-like structures formed by electrolytic hydrogenation. Physica E 43, 1262–1265.
Kahn, R., Fourme, R., André, D., Renaud, M., 1973. Crystal structures of cyclohexane I and II. Acta Crystallogr. B 29, 131–138.
Kavitha, G., Narayana, C., 2007. Raman spectroscopic investigations of pressure-induced phase transitions in *n*-Hexane. J. Phys. Chem. B 111, 14130–14135.
Kolesnikov, A., Kutcherov, V.G., Goncharov, A.F., 2009. Methane-derived hydrocarbons produced under upper-mantle conditions. Nat. Geosci. 2, 566–570.
Lobanov, S.S., Chen, P.-N., Chen, X.-J., Zha, C.-S., Litasov, K.D., Mao, H.-K., Goncharov, A.F., 2013. Carbon precipitation from heavy hydrocarbon fluid in deep planetary interiors. Nat. Commun. 4, 2446.
Luo, Z., Yu, T., Kim, K.-J., Ni, Z., You, Y., Lim, S., Shen, Z., Wang, S., Lin, J., 2009. Thickness-dependent reversible hydrogenation of graphene layers. ASC Nano 3, 1781–1788.
Mao, H.-K., Xu, J., Bell, P.M., 1986. Calibration of the ruby pressure gauge to 800 kbar under quasi-hydrostatic conditions. J. Geophys. Res. 91, 4673–4676.
Miller, F.A., Golob, H.R., 1964. The infrared and Raman spectra of cyclohexane and cyclohexane-d_{12}. Spectrochim. Acta 20, 1517–5130.
Nemanich, R.J., Solin, S.A., 1979. First- and second-order Raman scattering from finite-size crystals of graphite. Phys. Rev. B 20, 392–401.
Ogita, N., Yamamoto, K., Hayashi, C., Matsushima, T., Orimo, S., Ichikawa, T., Fujii, H., Udagawa, M., 2004. Raman scattering and infrared absorption investigation of hydrogen configuration state in mechanically milled graphite under H_2 gas atmosphere. J. Phys. Soc. Jpn. 73, 553–555.
Pardanaud, C., Martin, C., Roubin, P., Giacometti, G., Hopf, C., Schwarz-Selinger, T., Jacob, W., 2013. Raman spectroscopy investigation of the H content of heated hard amorphous carbon layers. Diam. Relat. Mater. 34, 100–104.
Pravica, M.G., Shen, Y., Nicol, M.F., 2004. High pressure Raman spectroscopic study of structural polymorphism in cyclohexane. Appl. Phys. Lett. 84, 5452–5454.
Reich, S., Thomsen, C., 2004. Raman spectroscopy of graphite. Philosophical Transactions of the Royal Society A 362, 2271–2288.
Rekhi, S., Dubrovinsky, L.S., Saxena, S.K., 1999. Temperature-induced ruby fluorescence shifts up to a pressure of 15 GPa in an externally heated diamond anvil cell. High. Temp.-High. Press. 31, 299–305.
Snyder, R.G., 1965. Group moment interpretation of the infrared intensities of crystalline *n*-paraffins. J. Chem. Phys. 42, 1744–1763.
Spanu, L., Donadio, D., Hohl, D., Schwegler, E., Galli, G., 2011. Stability of hydrocarbons at deep Earth pressures and temperatures. Procedings of the National Academy of Sciences of the United States of America 108, 6843–6846.
Yamaguchi, M., Serafin, S.V., Morton, T.H., Chronister, E.L., 2003. Infrared absorption studies of *n*-heptane under high pressure. J. Phys. Chem. B 107, 2815–2821.
Zerr, A., Serghiou, G., Boehler, R., Ross, M., 2006. Decomposition of alkanes at high pressures and temperatures. High Pres. Res. 26, 23–32.